

# Spectral linewidth of the Josephson Flux Flow Oscillator

V. P. Koshelets,<sup>1</sup> C. E. Mahaini,<sup>2</sup> J. Mygind,<sup>2</sup> M. R. Samuelsen,<sup>2</sup> and A. S. Sobolev<sup>1</sup>

<sup>1</sup>*Institute of Radio Engineering and Electronics, RAS, Moscow, Russia*

<sup>2</sup>*Department of Physics, B309, Technical University of Denmark, DK-2800 Lyngby, Denmark.*

(Dated: August 21, 2003)

The Flux Flow Oscillator is a long Josephson junction in which a DC bias current and a DC magnetic field maintain a unidirectional viscous flow of magnetic flux quanta. The linewidth of the electromagnetic radiation generated at the end boundary is theoretically given by the *lumped* junction expression. Experimentally, the linewidth deviates significantly both in magnitude and functional dependence. This disagreement has been a challenge for many years. We suggest a simple solution based on the assumption that the bias current creates an additional magnetic field in the junction.

PACS numbers: 85.25.Cp, 05.45.Yv, 74.50.+r

## INTRODUCTION

A Josephson junction inherently oscillates according to the Josephson voltage-phase relation  $\partial\phi/\partial t = (2\pi/\Phi_0)V(t)$ , where  $\phi$  is the phase difference between the macroscopic wave functions in the two superconductors forming the junction,  $\Phi_0 = h/2e$  is the flux quantum, and  $V(t)$  is the instantaneous voltage across the junction. When biased at a DC voltage  $V_{DC}$  the Josephson frequency is  $\nu_J = (1/\Phi_0)V_{DC}$ , where the pre-factor is  $\approx 484\text{GHz/mV}$ . With suitable electromagnetic coupling to the environment high frequency radiation may be emitted and the Josephson junction can be utilized as a tunable oscillator at millimeter and sub-millimeter wavelengths.

Theoretically the spectral linewidth  $\Delta\nu$  (FWHP, full width half power) of the *lumped* Josephson junction oscillator is given by [1, 2]

$$\Delta\nu = \pi \frac{R_d^2}{\Phi_0^2} S_I(0), \quad (1)$$

where  $R_d$  is the dynamic resistance in the bias point.  $S_I(0)$  is the power density of the *internal* low frequency current fluctuations including both thermal noise and shot noise [3]

$$S_I(0) = 2e\{I_{qp} \coth v + 2I_s \coth 2v\} \quad \text{with } v = \frac{eV}{2k_B T}, \quad (2)$$

where  $I_{qp}$  is the quasiparticle current and  $I_s$  is the superconducting pair current.  $T$  is the physical temperature. Eq. (1) comes from standard frequency modulation theory and the terms  $R_d^2$  and  $\Phi_0^2$  originate in the basic transformation of a current noise power spectrum to a voltage spectrum, and from the voltage spectrum to a frequency spectrum, respectively. Originally Eq. 2 was derived for a tunnel junction voltage biased at  $V$  but a similar formula may be obtained for the general case of arbitrary source impedance [4]. The pair current term accounts for the fact that the junction was coupled to a lossy resonator [1, 5]. Deviations from the assumed ideal "white" current noise power spectrum may be included as an effective temperature,  $T_{eff} > T$ .

Generally Eq. (1) applies to most both high- $T_c$  and low- $T_c$  Josephson oscillators e.g. point contacts and micro

bridges [3], short tunnel junctions, and resonant fluxon oscillators [6]. For well-characterized small tunnel junctions an observed difference (a pre-factor of less than 2) between theory and experiment can be accounted for by a modified basic current noise power spectrum (quantum effects). For some metallic weak links and high- $T_c$  junctions larger discrepancies (pre-factors of 2 to 100) have been observed. The resonant fluxon (soliton) oscillator has an extra pre-factor  $\frac{1}{4}$  because the (fluxon-antifluxon) reflection of a  $2\pi$ -kink results in a  $4\pi$  change of the phase difference leading to a modified Josephson frequency-phase relation. All these Josephson oscillators need only a single DC bias, usually supplied from a current source.

The Flux Flow Oscillator (FFO) differs from the other members of the Josephson oscillator family by needing also an applied DC magnetic field, usually generated by an external current in one of the junction electrodes or in a separate "control" line. Theoretically it has been shown [7, 10] that the linewidth of the ideal ("bare", see below) FFO also is given by the lumped junction expression Eq. (1). However, experimentally there is a substantial discrepancy (up to a factor 10) between the linewidth of real FFO's and that calculated using Eq. (1). Also a different functional dependence on  $R_d$  is found. This has been a puzzling problem for almost a decade [7–11]. In order to remedy the functional dependence and to obtain agreement with Eqs. (1,2) it has been tried in an empirical manner [12, 13] to include noise related to the control line current. Although the procedure provides good fits to our experiments over a wide parameter range, there is no theoretical justification for it. In fact, the implicit assumption [13] that the current fluctuations in the junction and in the control line are fully correlated, necessitates that the control line noise also originates in the internal current fluctuations.

## SINE-GORDON MODEL WITH BOUNDARIES

In a simple picture the dynamics of the FFO is a unidirectional viscous flow of mutually repulsive fluxons in a one-dimensional Josephson junction. The DC bias current,  $I$ , drives the fluxon chain while the applied DC magnetic field

from the current,  $I_{cl}$ , regulates the distance between the fluxons. Electromagnetic power may be extracted from the end of the junction where the fluxon chain collides with the boundary. In the frequency range 100-700 GHz it has been demonstrated that a standard Nb/Al<sub>2</sub>O<sub>3</sub>/Nb FFO can produce about 1μW, which is sufficient to pump an SIS mixer integrated on the same chip [14].

Using normalized units a long (length  $l$ ) and narrow (width  $w$ ) (rectangular) Josephson junction biased from a DC current supply is well modelled by the one-dimensional ( $l \gg w, w \ll 1$ ) perturbed sine-Gordon equation [6]  $\phi_{xx} - \phi_t = \sin \phi + \alpha \phi_t - \eta$ , where the normalized *overlap* current through the junction is  $\eta$  and  $\alpha$  is the normalized damping. Time  $t$  is normalized to the inverse maximum plasma frequency,  $\omega_0$ , length  $x$  to the Josephson penetration length,  $\lambda_J$ , currents to the maximum critical current,  $I_c$ , and magnetic fields to  $I_c \lambda_J$  which is half of the critical field,  $H_c = 2I_c \lambda_J$ , needed to force the first fluxon into the junction.

The normalized magnetic field  $\kappa_{1,2}$  at the two ends of the junction enters as the boundary condition

$$\phi_x(0,t) = \kappa_1 \quad \text{and} \quad \phi_x(l,t) = \kappa_2. \quad (3)$$

We assume that the field is in the plane of the junction and perpendicular to the  $x$ -direction. The total normalized current through the junction is

$$i = i_{ov} + i_{in} = w(\eta l + \kappa_2 - \kappa_1), \quad (4)$$

where  $i_{ov} = \eta w l = (\int_0^l w(x) \eta(x) dx)$  is the normalized *overlap* current,  $(\kappa_2 - \kappa_1)w = i_{in}$  is the *inline* part of the normalized junction current, and

$$\kappa = (\kappa_1 + \kappa_2)/2 \quad (5)$$

is the normalized magnetic field. The overlap fraction of the junction current is [15]

$$\chi = \frac{i_{ov}}{i_{in} + i_{ov}}. \quad (6)$$

The notation *overlap* and *inline* refers to the two idealized geometries for the long rectangular junction, where the DC bias current enters and leaves via the two long boundaries, or via the two narrow end boundaries, respectively.

The normalized DC I-V curve is given by

$$\omega = \omega(\eta, \kappa_1, \kappa_2) = \omega(i, \kappa), \quad (7)$$

where  $\omega = \langle \phi_t \rangle$  is the time average voltage across the junction. The I-V curve of a long low-damped overlap junction with homogeneous current distribution ( $\chi = 1$ ,  $\eta(x)$  constant) exhibits a very distinct step structure [16] with small dynamic resistance. Generally, both an inhomogeneous overlap current distribution ( $\eta(x)$ ) and/or some additional inline current supply ( $\chi < 1$ ) will alter the appearance of the structure. Higher damping broadens the structure and eventually turns it into the so-called flux flow step (FFS). For fixed bias current the voltage of the FFS is proportional to the magnetic field [16].

Until now we have discussed an *ideal* ("bare") junction where  $i$  and  $\kappa$  are *independent variables* with  $i$  proportional to the externally applied DC bias current  $I$  and  $\kappa$  proportional to the DC current  $I_{cl}$  in the control line. For later use we define two normalized dynamic resistances  $r_d$  and  $r_d^\kappa$  as partial derivatives of Eq. (7) with respect to the bias and control line current, respectively;

$$r_d = \frac{\partial \omega}{\partial i}, \quad r_d^\kappa = \frac{\partial \omega}{\partial \kappa} \frac{1}{w}, \quad (8)$$

where the dynamic resistance  $r_d^\kappa$  is derived from the current  $w\kappa$  equivalent to the magnetic field  $\kappa$ . The dynamic resistance,  $r_d$ , inserted (in unnormalized units) in Eq. (1) gives the linewidth of the "bare" FFO [7, 10].

## MAGNETIC FIELD GENERATED BY THE BIAS CURRENT

Now we consider the case where the external bias current generates a magnetic field in the junction. We assume that the normalized magnetic field in the junction consists of two contributions, an externally applied field:  $\kappa_{appl} = \beta i_{cl} \frac{1}{w}$  proportional to a DC current,  $i_{cl}$ , in the control line, and a field:  $-\sigma i$  proportional to the external DC bias current,  $i$ . As exemplified below the latter may be due to asymmetry of the junction and the way the bias current is fed to the junction.

$$\kappa w = \kappa_{appl} w - \sigma i = \beta i_{cl} - \sigma i. \quad (9)$$

Here  $\beta$  and  $\sigma$  are dimensionless factors determined by junction geometry and bias conditions. Now the *measured* normalized I-V curve is

$$\omega = \omega(i, \beta i_{cl} - \sigma i), \quad (10)$$

and correspondingly the *measured* normalized dynamical resistance is

$$r_d' = \left. \frac{d\omega}{di} \right|_{i_{cl}} = \frac{\partial \omega}{\partial i} + \frac{\partial \omega}{\partial \kappa} \frac{1}{w} (-\sigma) = r_d - \sigma r_d^\kappa. \quad (11)$$

We define a normalized control line dynamical resistance as

$$r_d^{cl} = \left. \frac{d\omega}{di_{cl}} \right|_i = \frac{\partial \omega}{\partial \kappa} \frac{1}{w} \beta = \beta r_d^\kappa. \quad (12)$$

i.e. the *measured* control line dynamical resistance  $(r_d^{cl})'$  is the same as before  $(r_d^{cl})' = r_d^{cl}$ . The normalized dynamic resistance,  $r_d$ , entering the linewidth expression Eq. (1) for the "bare" FFO is related to the *measured* dynamic resistances by

$$r_d = r_d' + \frac{\sigma}{\beta} (r_d^{cl})' = r_d' + K (r_d^{cl})', \quad (13)$$

where  $K = \frac{\sigma}{\beta}$  is the ratio between the two geometrical factors;  $\sigma$  for the external bias current and  $\beta$  for the external control line current. If the *measured* dynamical resistances

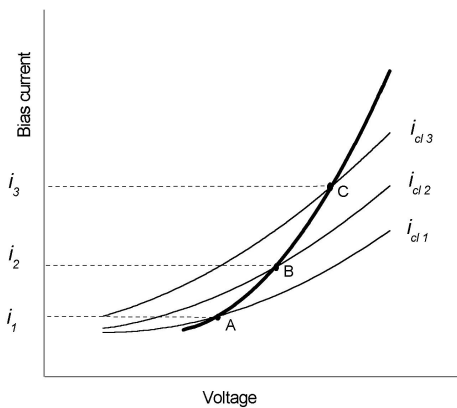


FIG. 1: Sketch showing how the real FFO I-V curve (thick full line) may be constructed if one knew the I-V curves of the ideal ("bare") junction, here represented by the three thin curves corresponding to three different control line currents ( $i_{cl1} > i_{cl2} > i_{cl3}$ ). A positive sign of  $K = \frac{\sigma}{\beta}$  (see Eq. (13)) is used, so that the magnetic field from the bias current makes the *measured* I-V curve steeper. For large  $K$ -values the I-V curve may have a *measured* dynamic resistance  $r'_d \leq 0$ .

as introduced in Eq. (13) are returned (in unnormalized units) to Eq. (1) the linewidth expression is replaced by

$$\Delta\nu = \pi \frac{(R'_d + KR_d^{cl})^2}{\Phi_0^2} S_I(0). \quad (14)$$

The derived equation contains just the empirical correction factor  $(R'_d + KR_d^{cl})^2$  which was used by Koshelets et al. [12] to obtain a good fit to Eqs. (1,2) with  $K$  as fitting parameter. With their particular junction layout the best fit was achieved with  $K \simeq 1$ . In fact a later measurement with a different bias configuration has given other  $K$ -values ( $K < 1$ ). Our more extensive measurements with other junction layouts will be published elsewhere.

All quantities in Eq. (14) can be measured with good accuracy. In a given bias point the free-running linewidth is measured with the FFO frequency-locked (by a frequency discriminator circuit) to a 400MHz reference using an on-chip integrated SIS junction as external harmonic mixer to down-convert the 100-700GHz signal so that it can be recorded with a spectrum analyser [11]. The corresponding two *measured* dynamical resistances  $(R_d)' = \frac{\Delta V}{\Delta I}$  and  $(R_d^{cl})' = (R_d^{cl}) = \frac{\Delta V}{\Delta I_{cl}}$  are calculated from the small voltage change  $\Delta V$  found when we increment the two currents by  $\Delta I$  and  $\Delta I_{cl}$ , respectively. The voltage change  $\Delta V$  is determined by measuring the frequency of the emitted radiation. Of course this measurement is done without frequency lock and thus the spectral line will slowly but erratically move on the spectrum analyser display due to drift and temperature variations. Since the uncertainty of the incremental currents  $\Delta I$  and  $\Delta I_{cl}$  can be reduced by averaging the dynamic resistances uncertainty is dominated by the voltage (frequency) measurement uncertainty, which is less

than  $\sim 5\text{nV}$  (corresponding to  $\sim 10\text{MHz}$ ). On the steep (Fiske step) structure in the I-V curve the free-running linewidth is of the order 100kHz.

As mentioned above the I-V curve Eq. (7) of the "bare" junction depends on the distribution of the junction current  $i$  - i.e. on the dependence of  $\eta(x)$  on  $x$ . Over the years several attempts have been made to reduce the linewidth by modifying the physical shape of the junction and of the superconducting electrodes near the junction, e.g. using the so-called "unbiased tail" as modelled by various current distributions [17–19]. From Eq. (14) and Fig. 1 it is obvious that a small value of the *measured* dynamic resistance  $R'_d$  in a real FFO not necessarily implies a narrow linewidth. This is valid only for  $K = 0$  corresponding to the ideal ("bare") junction. This mistake seems to have been carried over from the lumped junction scenario for over twenty years.

Looking at Fig. 1 one can obtain a situation where the real (measured) FFO I-V curve have negative values of the measured dynamic resistance  $R'_d$ . Such "back-bending" has been observed both experimentally and in our numerical simulations based on the sine-Gordon model. In the case where  $R'_d = 0$  in a given bias point the FFO linewidth measured here is solely due to internal bias current fluctuations conveyed via the  $K$  factor.

In conclusion, it is now clear that the spectral linewidth of real FFO's - contrary to the other Josephson oscillators including the ideal ("bare",  $K = 0$ ) FFO - in general is not given by the dynamic resistance of the measured DC I-V curve i.e. the long time average voltage  $V$  measured as function of the external DC bias current,  $I$ , for fixed applied magnetic field e.g. generated by an external current,  $I_{cl}$ , in a control line. Also the magnetic field generated by the external bias current must be taken into account.

## GENERAL CASE, EXAMPLES

In general for a given geometry we can write

$$\begin{aligned} w\kappa_1 &= \sigma_1 i + \beta_1 i_{cl} \\ w\kappa_2 &= \sigma_2 i + \beta_2 i_{cl} \\ \eta w l &= \sigma_3 i + \beta_3 i_{cl}. \end{aligned}$$

From Eq. (4) we get

$$\sigma_2 - \sigma_1 + \sigma_3 = 1 \quad \text{and} \quad \beta_2 - \beta_1 + \beta_3 = 0.$$

$\sigma_2 - \sigma_1$  is just the inline fraction  $1 - \chi$  of the junction current and  $\sigma_3$  is the overlap fraction  $\chi$ . From Eq. (5) we get

$$\kappa = \frac{\sigma_1 + \sigma_2}{2} i + \frac{\beta_1 + \beta_2}{2} i_{cl}.$$

This should be identical to Eq. (9) therefore we have

$$-\sigma = (\sigma_1 + \sigma_2)/2 \quad \text{and} \quad \beta = (\beta_1 + \beta_2)/2. \quad (15)$$

It is clear that  $\sigma$  can be ascribed to an asymmetric feed of the junction.  $K = \frac{\sigma}{\beta} = 1$  means that the bias current  $i$  and the

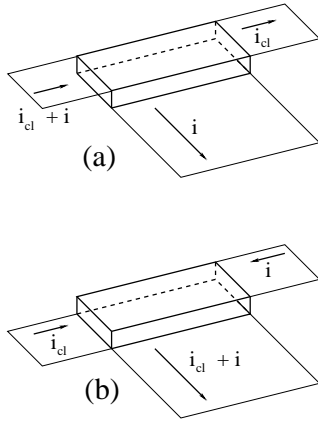


FIG. 2: Illustration of example 2, half inline; a)  $K = \frac{\sigma}{\beta} = \frac{1}{2}$ , half inline,  $\chi = \frac{1}{2}$ . b)  $K = \frac{\sigma}{\beta} = 1$ ,  $\chi = \frac{1}{2}$ . The figure is not to scale. In the superconducting thin-films currents flow with equal magnitude in top and bottom of the film

control line current  $i_{cl}$  (if equal) produce the same magnetic field. The situation is illustrated by three simple ideal examples which can be analyzed analytically. The external currents  $i$  and  $i_{cl}$  follow the same path on one side of the tunnel junction. The electrodes are superconducting thin-films assumed to be much thicker than the London penetration depth so the current flow is in a very thin layer in the top and bottom of the films.

**1) Pure overlap.** If the bias current  $i$  is purely overlap ( $\chi = 1$ ) there is no asymmetry in the bias current, therefore  $\sigma = 0$  and  $K = 0$ .

**2) Half inline.** In the half inline case ( $\chi = \frac{1}{2}$ ) there are two different cases. 2a) First the situation in Fig. 2a. Simple considerations give

$$\sigma_2 \simeq \sigma_3 \simeq \frac{1}{2}, \quad \beta_2 = \beta_1 = \frac{1}{2}, \quad \text{and} \quad \sigma_1 \simeq \beta_3 \simeq 0,$$

or  $\beta = \frac{1}{2}$  and  $\sigma = \frac{1}{4}$  and therefore  $K = \frac{1}{2}$ . 2b) The other situation with half inline is shown in Fig. 2b. Here

$$\sigma_2 \simeq \sigma_3 \simeq \beta_1 \simeq \beta_3 \simeq \frac{1}{2} \quad \text{and} \quad \sigma_1 \simeq \beta_2 \simeq 0,$$

or  $\beta = \frac{1}{4}$  and  $\sigma = \frac{1}{4}$  and therefore  $K = 1$ .

**3) Pure inline.** If the bias current is purely inline ( $\chi = 0$ ) there are two cases. Let  $i_{cl}$  flow in the bottom film. If  $i$  flows into one end of the junction from the bottom film and leaves the junction through the top film and the other end of the junction (Fig. 3a) there is no asymmetry in the current,  $\beta = \frac{1}{2}$  therefore  $\sigma = 0$  and  $K = 0$ . If the bias current  $i$  leaves the junction from the same end as it enters (Fig. 3b) the asymmetry in the current is  $\sigma = \frac{1}{2}$ ,  $\beta = \frac{1}{2}$  and therefore  $K = 1$ .

The work was supported in part by the RFBR project 03-02-16748, INTAS project 01-0367, ISTS project 2445, the Danish Natural Science Foundation and the Hartmann Foundation.

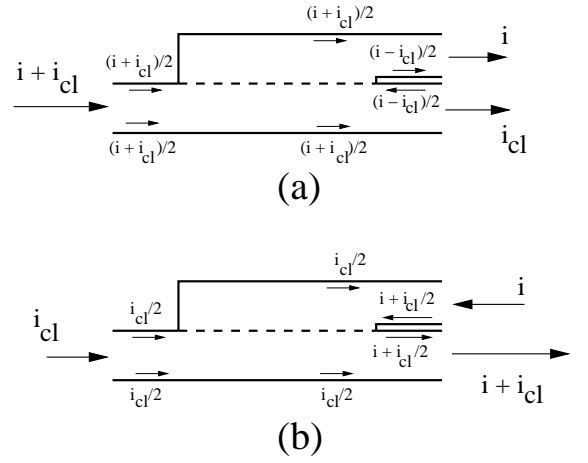


FIG. 3: Illustration to example 3. Pure inline ( $\chi = 0$ ). The figure is not to scale. The total current in each superconducting thin-film is the sum of the currents flowing in the top and bottom of the film as indicated. The dashed line indicates the tunnel barrier. Two cases; a)  $\sigma = 0$  and therefore  $K = 0$  and b)  $\sigma = \frac{1}{2}$ ,  $\beta = \frac{1}{2}$  and therefore  $K = 1$ .

- 
- [1] D. Rogovin and D.J. Scalapino, *Ann. of Phys.* **86**, 1, (1974)
  - [2] K.K. Likharev, *Dynamics of Josephson junctions and circuits*, New York. Gordon and Breach Science Publishers, 1986.
  - [3] A.J. Dahm, A. Denenstien, D.N. Langenberg, W.H. Parker, D. Rogovin, and D.J. Scalapino, *Phys. Rev. Lett.* **22**, 1416 (1969).
  - [4] A.B. Zorin, *Physica B*, **108**, 1293 (1981)
  - [5] M.J. Stephen, *Phys. Rev. Lett.* **21**, 1629 (1968).
  - [6] E. Jørgensen, V.P. Koshelets, R. Monaco, J. Mygind, M.R. Samuelsen, and M. Salerno, *Phys. Rev. Lett.* **49**, 1093 (1982).
  - [7] M. Salerno, M.R. Samuelsen, and A.V. Yulin, *Phys. Rev. Lett.* **86**, 5397 (2001).
  - [8] A.V. Ustinov, H. Kohlstedt, and P. Henne, *Phys. Rev. Lett.* **77**, 3617 (1996).
  - [9] A.A. Golubov, B.A. Malomed, and A.V. Ustinov, *Phys. Rev.* **B54**, 3047 (1996).
  - [10] A.P. Betenev and V.V. Kurin, *Phys. Rev.* **B56**, 7855 (1997).
  - [11] V.P. Koshelets, S.V. Shitov, A.V. Shchukin, L.V. Filippenko, J. Mygind, and A.V. Ustinov, *Phys. Rev.* **B56**, 5572 (1997).
  - [12] V.P. Koshelets, P.N. Dmitriev, A.B. Ermakov, A.S. Sobolev, A.M. Baryshev, P.R. Wesselius, and J. Mygind, *Supercond. Sci. Technol.* **14**, 1040 (2001).
  - [13] A.L. Pankratov, *Phys. Rev.* **B65**, 054504 (2002).
  - [14] V.P. Koshelets, A. Shchukin, I.L. Lapytskaya, and J. Mygind, *Phys. Rev.* **B51**, 6536 (1995).
  - [15] M.R. Samuelsen and S.A. Vasenko, *J. Appl. Phys.* **57**, 110 (1984).
  - [16] M. Cirillo, N. Grønbech-Jensen, M. R. Samuelsen, M. Salerno, and G. Verona Rinati, *Phys. Rev.* **B58**, 12 377 (1998).
  - [17] A.L. Pankratov, *Phys. Rev.* **B66**, 134526 (2002).
  - [18] T. Nagatsuma *et al.* *J. Appl. Phys.* **54**, 3302 (1983), **56**, 3284 (1984), **58**, 441 (1985), and **63**, 1130 (1988).
  - [19] Y.M. Zhang and P.H. Wu, *J. Appl. Phys.* **69**, 4703 (1990).